Theory of spin splitting in $Ga_{1-x}Al_xAs$ parabolic quantum wells controlled by an electric field

P. Pfeffer and W. Zawadzki
Institute of Physics, Polish Academy of Sciences, Al.Lotnikow 32/46, 02–668 Warsaw, Poland
(Received 14 February 2005; revised manuscript received 2 May 2005; published 14 July 2005)

The five-level $\mathbf{k}\cdot\mathbf{p}$ model for $Ga_{1-x}Al_xAs$ parabolic quantum wells, characterized by the continuously varying chemical composition x, is used to calculate the effective spin g^* factor of conduction electrons. The theory with no adjustable parameters agrees well with the experimental data of Salis *et al.* [Nature **414**, 619 (2001)].Both negative and positive spin g^* values are described, as well as their dependence on an external electric field. The Bychkov-Rashba spin splitting due to inversion asymmetry of the structures caused by electric bias is calculated and shown to give negligible contribution to the g^* values.

DOI: 10.1103/PhysRevB.72.035325 PACS number(s): 73.40.Cg, 73.50.Jt, 73.61.Ey

I. INTRODUCTION

Spin systems in semiconductors are considered to be among the promising ones for future quantum computers.[1–3] Such systems often represent two-level quantum states (qubits) and some of them are sufficiently weakly coupled with the environment to assure long spin decoherence times. In order to process quantum information one needs to manipulate fast and coherently the local spins. The most natural way to control the spin splitting is to apply external magnetic fields. This, however, requires their precise control at small length scales which is not easy. Salis *et al.*[4] demonstrated that one can control the spin splitting and spin coherence using an external electric field. This was achieved employing $Ga_{1-x}Al_xAs$ quantum wells (QWs) and manipulating the electron wave functions within such wells. In particular, since the bulk GaAs is characterized by a small and negative spin g^* factor and with the growing Al content x the g^* factor becomes positive, it was possible to do experiments near the vanishing spin splitting and to have no spin precession at specific electric fields. The experiments of Ref. 4 were interpreted using a simple phenomenological theory. Also, it was necessary to lower all theoretical values of g^* by 0.05 in order to obtain the agreement with the experiments. It is the purpose of the present work to provide a description of the data of Salis *et al.* with an adequate theoretical formalism and to employ only parameters determined by other measurements.

It was shown some time ago that, since bulk GaAs is a medium gap semiconductor, the description of its conduction band requires the use of a five-level (5L) $\mathbf{k}\cdot\mathbf{p}$ model.[5,6] This model describes the effective mass m^* and the effective Landé spin factor g^* at the conduction band edge and its dependence on the electron energy $\mathcal{E}$ within the band due to the band's nonparabolicity. The 5L $\mathbf{k}\cdot\mathbf{p}$ model was subsequently adopted to III-V heterojunctions, in which the mass m^* and the factor g^* can depend not only on the energy $\mathcal{E}$ but also on the spacial variable along the growth direction.[7,8] It is this approach that we will use below to describe $Ga_{1-x}Al_xAs$ alloys and their heterostructures with continuously variable x.

The problem of g^* factor in QWs was treated theoretically by other authors.[9–11] In particular, it was predicted and verified experimentally[12] that, in sufficiently narrow QWs, the $g^*_{\|}$ value for a magnetic field $\mathbf{B}$ parallel to the growth direction $\mathbf{z}$ differs from the value of $g^*_{\perp}$ for $\mathbf{B}\perp\mathbf{z}$. In the following we will be concerned only with the $\mathbf{B}\|\mathbf{z}$ case. We use a somewhat different approach than that employed in Refs. 9–11. First, we use the 5L $\mathbf{k}\cdot\mathbf{p}$ model, adequate for the GaAs-type materials, whereas Refs. 9–11 employed the Kane (3L) model. Second, Refs. 9–11 considered specific QWs (mostly rectangular), whereas our formulation can handle QWs of arbitrary shape. Finally, Refs. 9–11 employed expansions in terms of the $\mathbf{k}\cdot\mathbf{p}$ perturbation, while we treat the coupled $\mathbf{k}\cdot\mathbf{p}$ equations exactly including the well potential $V(z)$ and project the problem onto the conduction band by substitution. In this scheme the effective mass $m^*(z)$ and the spin factor $g^*(z)$ depend on the spatial variable z via the well potential $V(z)$ and the band offsets. This approach is very well suited to the description of experimental work of the type carried out by Salis *et al.*

Our paper is organized in the following way: In Sec. II we present the general theory for the effective mass and the g factor in the case of the variable band parameters. In Sec. III we treat the specific system used by Salis *et al.*, present the results and discuss them. Section IV describes the spin splitting caused by the structure inversion asymmetry. The paper concludes with a summary.

II. THEORY

We consider $Ga_{1-x}Al_xAs$ structures used in the experiments of Salis *et al.* Parabolic potential wells used in that work were obtained varying the alloy content x as a function of the position z. This means that the energy gap and other band parameters are functions of z. As mentioned in the Introduction, in our description we use the adequate five-level $\mathbf{k}\cdot\mathbf{p}$ model for the band structure of the alloys. The 5L model for bulk $Ga_{1-x}Al_xAs$ is shown in Fig. 1. This model explicitly takes into account 14 bands arising from the Γ^v_7, Γ^v_8 (double degenerate), Γ^c_6, Γ^c_7, Γ^c_8 (double degenerate) levels, times the double spin degeneracy, and treats the distant (upper and lower) levels as a perturbation. Below we use the spherical version of the 5L model (with the matrix element $Q=0$). The nonspherical case is considered in the Appendix.

We have to determine first the parameters of the model. According to our scheme the bulk electron effective mass m^*

 ©2005 The American Physical Society

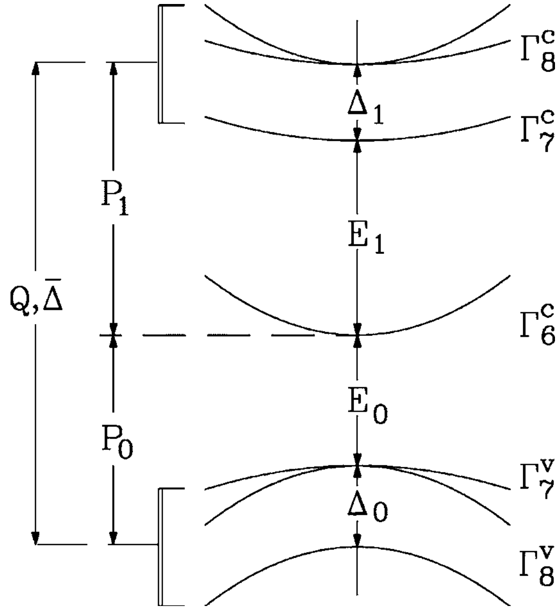

FIG. 1. Five-level model of the band structure at the Γ point for GaAs-type semiconductors. Level symmetries Γ_i, energy gaps E_i, and spin-orbit energies Δ_i are indicated. The arrows indicate which levels are coupled by the matrix elements of momentum (P_0, P_1, Q) and of the spin-orbit interaction $(\bar{\Delta})$. The zero of energy is chosen at the Γ_6^c conduction band edge.

and the electron spin g^* value at the conduction band edge are (see Ref. 5)

$$\frac{m_0}{m_0^*} = 1 + C - \frac{1}{3}\left[E_{P_0}\left(\frac{2}{E_0} + \frac{1}{G_0}\right) + E_{P_1}\left(\frac{2}{G_1} + \frac{1}{E_1}\right) + \frac{4\bar{\Delta}}{3}\sqrt{E_{P_0}\cdot E_{P_1}}\left(\frac{1}{E_1 G_0} - \frac{1}{E_0 G_1}\right)\right] \tag{1}$$

and

$$g_0^* = 2 + 2C' + \frac{2}{3}\left[E_{P_0}\left(\frac{1}{E_0} - \frac{1}{G_0}\right) + E_{P_1}\left(\frac{1}{G_1} - \frac{1}{E_1}\right) - \frac{2\bar{\Delta}}{3}\sqrt{E_{P_0}\cdot E_{P_1}}\left(\frac{2}{E_1 G_0} + \frac{1}{E_0 G_1}\right)\right], \tag{2}$$

where $G_0 = E_0 + \Delta_0$ and $G_1 = E_1 + \Delta_1$. The involved gaps and spin-orbit energies are defined in Fig. 1. The interband matrix elements of momentum,

$$P_0 = \frac{-i\hbar}{m_0\Omega}\langle S|p_x|X\rangle, \tag{3}$$

$$P_1 = \frac{-i\hbar}{m_0\Omega}\langle S|p_x|X'\rangle, \tag{4}$$

are given by means of the energies $E_{P_0} = 2m_0P_0^2/\hbar^2 = 27.86$ eV, $E_{P_1} = 2m_0P_1^2/\hbar^2 = 2.36$ eV, while the interband spin-orbit parameter $\bar{\Delta} = -0.061$ eV is

TABLE I. Far-band contributions to the effective mass m_0/m_0^* and the g^* value in $Ga_{1-x}Al_xAs$ alloys for three values of the chemical composition x, see text.

x	C	C'_{WH}	C'_{Ch}
0.0	−2.23	−0.025	−0.025
0.14	−1.57	−0.034	−0.009
0.40	−2.61	−0.076	+0.016

$$\bar{\Delta} = \frac{-i3\hbar}{4m_0^2c^2}\langle X|(\nabla V_0 \times \mathbf{p})_y|Z'\rangle, \tag{5}$$

(see Ref. 5). Finally, C and C' are distant band contributions to m_0/m_0^* and g_0^*, respectively. In the following we assume, in agreement with the standard procedure, that E_{P_0}, E_{P_1}, and $\bar{\Delta}$ are constant, while all other parameters in Eqs. (1) and (2) are functions of the composition x.

The x dependence of $E_0(x)$ and $G_0(x)$ are known from Refs. 13,14,

$$E_0(x) = -(1.5194 + 1.36x + 0.22x^2) \text{ eV}, \tag{6}$$

$$G_0(x) = -(1.8594 + 1.229x + 0.291x^2) \text{ eV}. \tag{7}$$

For the x dependence of $E_1(x)$ and $G_1(x)$ we take linear interpolations between the corresponding values for GaAs and AlAs,

$$E_1(x) = (2.969 + 0.971x) \text{ eV}, \tag{8}$$

$$G_1(x) = (3.14 + 0.98x) \text{ eV}. \tag{9}$$

The above relations can be inserted into Eqs. (1) and (2) to obtain the x dependence of m_0/m_0^* and g_0^*. There remain the unknown far-band corrections $C(x)$ and $C'(x)$. However, the experimental dependence of m_0/m_0^* is known from the Shubnikov–de Haas data[15]

$$\frac{m_0}{m_0^*} = 0.0657 + 0.0174x + 0.145x^2. \tag{10}$$

Comparing the x dependence of m_0/m_0^* described by Eq. (1) [supplemented by Eqs. (6)–(9)] we can determine $C(x)$. The results for three values of x are quoted in Table I.

We apply the same procedure to determine $C'(x)$ in Eq. (2). The x dependence of $g_0^*(x)$ is described by Eq. (2) supplemented by Eqs. (6)–(9). On the other hand, there exists in the literature two somewhat different measurements of $g_0^*(x)$ for $Ga_xAl_{1-x}As$ alloys. They can be described by numerical fits. According to the data of Chadi *et al.*[16] (obtained at 77 K)

$$g_{Ch}^* = -0.44 + 4.55x - 3.5x^2, \tag{11}$$

whereas according to Weisbuch and Hermann[17] (obtained at 4 K)

$$g_{WH}^* = -0.44 + 4.25x - 3.9x^2. \tag{12}$$

Comparing Eqs. (2) and (11) one can determine one set of $C'_{Ch}(x)$, while the same procedure for Eqs. (2) and (12) gives

the second set $C'_{\mathrm{WH}}(x)$. Both are indicated in Table I. It can be seen that, both in case of the mass and of the g^* value, the distant band corrections are much smaller than the principal contributions of the five levels. This confirms the adequacy of the 5L model.

The electrons are confined in a potential well. As a consequence, the measured g^* value is given by an average of $g^*(z)$ calculated using the electron wave function in the well. In order to find the wave function for the conduction band one should solve the 5L model which represents the set of 14 coupled differential equations for the envelope functions f_i.[7] The external potential appears on the diagonal of the set. However, within the spherical approximation (which amounts to putting the matrix element $Q=0$, see Fig. 1) we can solve the set by substitution expressing $f_3, \ldots, f_{14}$ by f_1 and f_2, where f_1 and f_2 are the envelope functions corresponding to the spin-up and spin-down conduction states, respectively.

The resulting differential equation for f_n^+ and f_n^- functions is

$$\left[-\frac{\hbar^2}{2}\frac{\partial}{\partial z}\frac{1}{m^*(z)}\frac{\partial}{\partial z}+\frac{\hbar eB}{m^*(z)}\left(n+\frac{1}{2}\right)\pm\frac{\mu_B B g^*(z)}{2}+V_c(z)+eFz\right]f_n^{\pm}(z)=\mathcal{E}f_n^{\pm}(z), \quad (13)$$

where the effective mass is

$$\frac{m_0}{m^*(z)}=1+C(z)-\frac{1}{3}\left[E_{P_0}\left(\frac{2}{\tilde{E}_0}+\frac{1}{\tilde{G}_0}\right)+E_{P_1}\left(\frac{2}{\tilde{G}_1}+\frac{1}{\tilde{E}_1}\right)+\frac{4\bar{\Delta}}{3}\sqrt{E_{P_0}\cdot E_{P_1}}\left(\frac{1}{\tilde{E}_1\tilde{G}_0}-\frac{1}{\tilde{E}_0\tilde{G}_1}\right)\right], \quad (14)$$

and the g^* factor is

$$g^*(z)=2+2C'(z)+\frac{2}{3}\left[E_{P_0}\left(\frac{1}{\tilde{E}_0}-\frac{1}{\tilde{G}_0}\right)+E_{P_1}\left(\frac{1}{\tilde{G}_1}-\frac{1}{\tilde{E}_1}\right)-\frac{2\bar{\Delta}}{3}\sqrt{E_{P_0}\cdot E_{P_1}}\left(\frac{2}{\tilde{E}_1\tilde{G}_0}+\frac{1}{\tilde{E}_0\tilde{G}_1}\right)\right]. \quad (15)$$

Here $\tilde{E}_i(z)=E_i(z)-\mathcal{E}+V_c(z)+eFz$, $\tilde{G}_i(z)=G_i(z)-\mathcal{E}+V_c(z)+eFz$, and F is an external electric field. The index n in $f_n^{\pm}$ functions corresponds to the nth Landau level in Eq. (13). In addition to the z dependencies resulting from the x dependencies in Eqs. (1) and (2), the effective mass (14) and the g^* value (15) depend on the potential $V_c(z)+eFz$ and on the eigenenergy $\mathcal{E}$. This is a consequence of band's nonparabolicity, as shown in Refs. 7 and 8. Because m^* and g^* depend on the eigenenergy, Eq. (13) must be solved self-consistently. In practice this is done by putting a fixed value of $\mathcal{E}$ both in $m^*(\mathcal{E},z)$, $g^*(\mathcal{E},z)$ and as the eigenvalue on the RHS of Eq. (13), and checking whether this value satisfies Eq. (13) with the boundary conditions $f_n^{\pm}\to 0$ at $z=\pm\infty$.

In Eq. (13) we omit in the first approximation the spin term since we are concerned with very small spin splittings (see below). This approximation is verified in Sec. IV. Also, we consider only the lowest $n=0$ Landau level because we deal with very low electron densities ($n_{2D}\approx 10^{10}$ cm^{-2}), so that all electrons occupy the ground state. It is to be noted that formulas (14) and (15) are valid also in the barriers, that is in the classically forbidden regions.

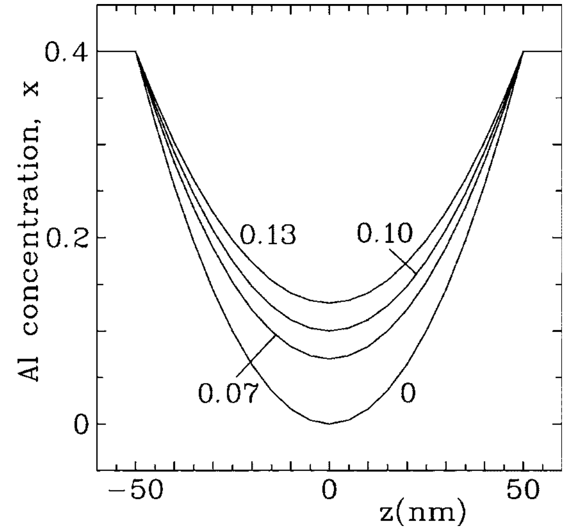

FIG. 2. Conduction band potential profiles for four $Ga_{1-x}Al_xAs$ parabolic quantum wells with variable Al content x, as used by Salis *et al.* (Ref. 4). The numbers indicate minimum Al content x_0 (at the band's minimum) for a given sample.

Once the electron wave function $f_0(z)$ is found, the average value of g^* is obtained,

$$g^*_{\mathrm{av}}=\langle f_0|g^*(z)|f_0\rangle. \quad (16)$$

In the coupled-band scheme the total wave function for the conduction band has more than one component but, because the gap in the GaAs-type materials is not narrow, the other (small) components may be safely neglected.

III. RESULTS AND DISCUSSION

The potential profiles for the conduction band in samples used by Salis *et al.* are shown in Fig. 2. In order to translate the x content into the energies we use the relation $\Delta V_c=0.80x$(eV) for $0\le x\le 0.45$.[18] The profiles are described by the parabolas $V_c(z)=V_0+bz^2$, where $b=(V_m-V_0)/(a/2)^2$ is obtained from the well parameters. In all cases $a=100$ nm and $V_m=0.32$ eV while the minimum potential V_0 is different for each sample. Since the structures of Salis *et al.* had few electrons ($n_{2D}\approx 10^{10}$ cm^{-2}), the free charges did not substantially affect the well potential. The profiles of all bands within the 5L model for the quantum well with the minimum value $x_0=0$, are shown in Fig. 3. If one applies an external electric field, the potential well is still parabolic but its minimum is shifted to a different alloy composition x'_0, which directly influences the $g^*(z)$ function and, in turn, the value of g^*_{av}, see Fig. 4.

We solved numerically Eq. (13) both without the electric field and with the electric field F. In both cases the electrons are located in a parabolic potential well. Still, because of the

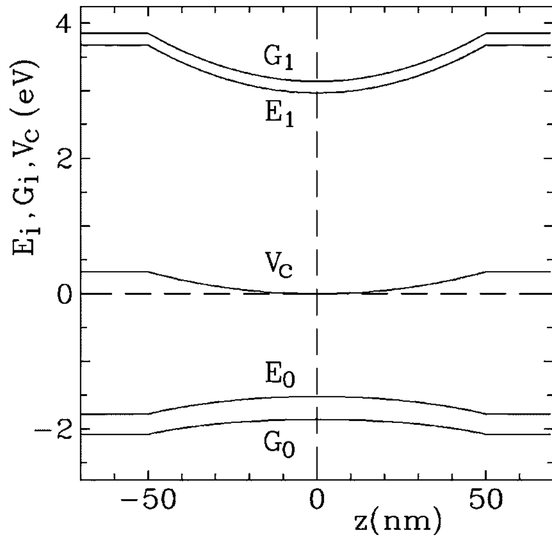

FIG. 3. Energy profiles of five levels at the Γ point for the $Ga_{1-x}Al_xAs$ sample with $x_0=0$ along the growth direction z, as determined from the dependencies of band parameters on the Al content x.

$m^*(z)$ dependence and the "kinks" of the potential at finite z values (see Fig. 4) the resulting wave functions are not exactly those of the harmonic oscillator's. The potential profiles for the quantum well with $x_0=0$ in case of $F=0$ and $F=3.64\times10^4$ V/cm are shown in Fig. 4. The same figure shows the calculated wave functions for the two cases.

Finally, Fig. 5 shows our theoretical values of g^*_{av} compared to the experimental findings of Salis *et al.* It was found in Ref. 4 that the experimental data are symmetric around the bias value of $U_0\approx1.5$ V, which seems to be the "built-in" voltage. Clearly, our theoretical results are symmetric around the bias voltage $U_{tot}=0$. This is taken into account in Fig. 5, on the lower abscissa where we put the experimental gate voltage U_g and on the upper one $U_{tot}=U_g+U_0$. We show two

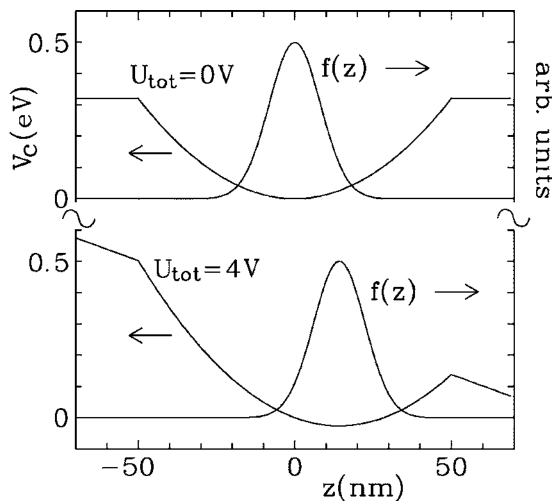

FIG. 4. Potential profile of the conduction band for the sample with $x_0=0$ in the absence of an external electric field (upper part) and with the electric bias of 4 V (lower part). The calculated electron wave functions for the two cases are shown.

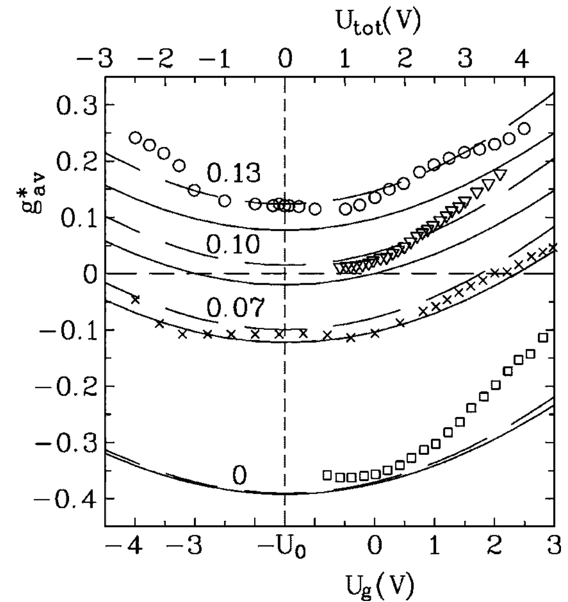

FIG. 5. Theoretical spin g^* factors of conduction electrons in four $Ga_{1-x}Al_xAs$ parabolic quantum wells, as used by Salis *et al.* (Ref. 4), versus external electric bias. The solid lines are calculated using bulk $g^*_{WH}(x)$ data of Weisbuch and Hermann (Ref. 17), the dashed lines are the same using $g^*_{Ch}(x)$ data of Chadi *et al.* (Ref. 16). Various symbols show the experimental results of Salis *et al.*

sets of theoretical curves. The dashed lines are calculated according to the $g^*_{Ch}(x)$ experimental values of Chadi *et al.*,[16] while the solid lines are the same but using the g^*_{WH} experimental values of Weisbuch and Hermann,[17] see Sec. II. The dashed lines are systematically higher than the solid ones, which is due to the fact that with growing x the experimental values of g^*_{Ch} are higher than g^*_{WH}. This agrees with the temperature dependence of $g^*(T)$ in GaAs, as investigated in Ref. 19, since the values of g^*_{Ch} were measured at $T=77$ K, while g^*_{WH} were determined at $T=4$ K. Thus the data of Weisbuch and Hermann should correspond better to the experiments of Salis *et al.* because both were carried out at low temperatures.

As for the comparison of the theory with experiment, it is on the whole very good, with two small discrepancies. First, for the sample with the highest Al content ($x_0=0.13$) the experimental data are slightly higher than the theoretical solid line. Second, for the samples with $x_0=0$ and $x_0=0.10$ the experimental dependencies of g^* on the voltage are steeper than the theoretical ones. It can be seen, however, that the other two samples exhibit weaker $g^*(U_g)$ dependencies, so that this problem is clearly of the experimental or technological nature. It should be emphasized that our good theoretical fit is obtained without any adjustable parameters and all the used parameter values were established by independent experiments. In fact, it is impressive that the different experiments on $Ga_{1-x}Al_xAs$ alloys used in the present analysis give results corresponding so well to each other.

It is of interest to compare the results of the five-level model for the band structure of $Ga_{1-x}Al_xAs$ with those of a simpler three-level model. In principle, the 5L model is necessary for the GaAs-type materials since, as follows from

Fig. 3, the energy distance from the Γ_6 conduction band to the higher conduction bands is $E_1=3$ eV, which is only twice larger than the fundamental energy gap $E_0=1.5$ eV. As we showed earlier,[5] the differences between the two models become appreciable when the energy of conduction electrons increases. In our scheme we adjust the far-band contributions to the effective mass and the g^* value to obtain the same band-edge values. Consequently, the far-band contributions for the 3L model are larger than those for the 5L model. It turns out that, since the subband energies in question are quite low ($\mathcal{E}\approx 13$ meV), so that the nonparabolic effects are very small, the resulting theoretical g^* values according to the 3L model are practically the same as those given above. However, it should be emphasized again that the 5L model is necessary for GaAs since it uses reasonable values of P_0 and P_1 matrix elements and it gives the band's anisotropy observed experimentally.

Finally, we estimated the effects of free carrier density induced by interband optical excitations on the self-consistent potential of quantum wells in the experiments of Salis *et al.* When there is no electric bias there is no net charge since the interband excitation creates equal numbers of electrons and holes. When an external voltage is applied, the charge densities of electrons and holes are shifted with respect to each other. We calculated in a self-consistent procedure the effect of $n_{2D}=10^{10}$ cm^{-2} electrons at the highest bias of 3 V for the sample 0.13 (see Fig. 5). It turns out that, while the modification of the potential and the corresponding subband energy are not negligible, the resulting average g^* values are practically the same. The change of g^* for the above case is $\Delta g^*\approx 10^{-4}$ between the parabolic potential and the self-consistent potential. This can be understood by observing that the g^* value depends on $1/(E_0-\mathcal{E}+V_c)$ [see Eq. (15)] in which, for GaAs, the value of $\mathcal{E}-V_c$ is three orders of magnitude smaller than E_0.

IV. BYCHKOV-RASHBA SPIN SPLITTING

Once an external electric field is applied to the symmetric parabolic QWs the structure inversion asymmetry (SIA) appears and, as a result, there arises the spin splitting of subband energies at $B=0$, called the Bychkov-Rashba splitting.[20] There exists also the spin splitting due to the bulk (or crystal) inversion asymmetry (BIA) (sometimes called the Dresselhaus splitting[21]), but the latter is present both for $F=0$ and $F\neq 0$. The properties of SIA and BIA spin splittings were reviewed by Zawadzki and Pfeffer.[22] In the present section we estimate the SIA spin splitting in order to check whether it can influence our theoretical results for the g^* values presented above. We do not give here the derivation of the corresponding formulas, they can be found in Refs. 22,23.

The SIA spin splitting of the conduction subband at $B=0$ is

$$\Delta E_{SIA} = 2\alpha k_F, \tag{17}$$

where

$$\alpha = \frac{1}{2}\langle f|\frac{\partial \eta}{\partial z}|f\rangle, \tag{18}$$

in which

$$\eta(z) = \frac{2}{3}\left[P_0^2\left(\frac{1}{\tilde{E}_0} - \frac{1}{\tilde{G}_0}\right) + P_1^2\left(\frac{1}{\tilde{G}_1} - \frac{1}{\tilde{E}_1}\right) + - \frac{2\bar{\Delta}}{3}P_0P_1\left(\frac{1}{\tilde{E}_0\tilde{G}_1} + \frac{2}{\tilde{E}_1\tilde{G}_0}\right)\right]. \tag{19}$$

One should note that, while the averaging in Eq. (18) is carried out with the use of the wave function for the Γ_6^c conduction subband, the derivative $\partial\eta/\partial z$ involves the band profiles of the valence and the upper conduction bands, see Fig. 3. This problem is discussed in detail in Ref. 22. Inserting the experimental values of $k_F=2.5\times 10^5$ cm^{-1}($n_{2D}=10^{10}$ cm^{-2}) and calculating the wave function f_0 for $U_{tot}=2$ V (cf. Fig. 4) we obtain for the sample with $x_0=0.10$ the value of $\Delta E_{SIA}=7.3\times 10^{-3}$ meV. If the spin splitting due to SIA did not depend on an external magnetic field, the above splitting would correspond to the field of $B=6$ T to the change of the g^* value $\Delta g^*\approx 0.0001$, i.e., it would be negligible compared to our estimated value of $g^*_{av}=0.0139$. In fact, as we showed elsewhere,[22,23] ΔE_{SIA} is a decreasing function of an external magnetic field. The subband energies in the presence of **B** parallel to the growth direction (including the SIA splitting) are

$$E_n^+ = \frac{\varepsilon_n^+ + \varepsilon_{n+1}^-}{2} - \left[\left(\frac{\varepsilon_{n+1}^- - \varepsilon_n^+}{2}\right)^2 + \frac{2}{L^2}(\alpha_n^+)^2(n+1)\right]^{1/2}, \tag{20}$$

$$E_n^- = \frac{\varepsilon_n^- + \varepsilon_{n-1}^+}{2} + \left[\left(\frac{\varepsilon_n^- - \varepsilon_{n-1}^+}{2}\right)^2 + \frac{2}{L^2}(\alpha_n^-)^2 n\right]^{1/2}, \tag{21}$$

where

$$\alpha_n^+ = \frac{1}{2}\langle f_n^+|\frac{\partial \eta}{\partial z}|f_{n+1}^-\rangle, \tag{22}$$

$$\alpha_n^- = \frac{1}{2}\langle f_{n-1}^+|\frac{\partial \eta}{\partial z}|f_n^-\rangle, \tag{23}$$

in which $f_n^\pm$ and $\varepsilon_n^\pm$ are the corresponding envelope functions and energies of the spin-up and spin-down Landau levels n without the SIA splitting, as obtained from Eq. (13). We first calculate the energies without the SIA splitting. To this end we solve numerically Eq. (13) including this time the spin term with the spin factor $g^*(\mathcal{E},z)$ given by Eq. (15). For the sample with $x_0=0.10$ at the external fields $B=6$ T and $F=1.82\times 10^4$ V/cm we calculate ε_0^+ and ε_0^-, resulting in $g^*=0.0143$. This verifies our approximation used above, which gave the same parameters $g^*_{av}=0.0139$.

Now we can calculate the spin splitting including the SIA contribution. For the lowest Landau level $n=0$ there is $f_{n-1}=0$, so that the E_0^- energy is not affected by the SIA mechanism. Calculating the correction to the E_0^+ level we obtain the modified spin factor at $B=6$ T to be $g^*=0.0142$. Thus the

SIA mechanism gives negligible contribution to the theoretical g^* values shown in Fig. 5. This is true also for the smallest g^* value of the sample with $x_0=0.10$.

We estimated the Bychkov-Rashba splitting according to the 3L model as well. The SIA modifications to the g^* values are again negligible, the decisive factor being the relatively high magnetic field $B=6$ T, which suppresses the Bychkov-Rashba splitting (see the analysis in Ref. 24).

V. SUMMARY

Using the five-level $\mathbf{k}\cdot\mathbf{p}$ model for GaAs-type semiconductors in the presence of external magnetic and electric fields we described the spin splitting of conduction subbands in $Ga_{1-x}Al_xAs$ parabolic quantum wells grown by a continuous variation of the Al content x. The theory, having no adjustable parameters, agrees well with the experimental findings of Salis *et al.* Both negative and positive spin g^* values are obtained. The theory correctly accounts for the variation of g^* values on external electric field. The Bychkov-Rashba spin splitting, arising from inversion asymmetry introduced by the electric bias, is calculated and shown to give negligible contribution to the calculated g^* values at low electron densities.

ACKNOWLEDGMENT

This work was supported in part by The Polish Ministry of Sciences, Grant No. PBZ-MIN-008/PO3/2003.

APPENDIX

The growth direction of QWs used by Salis *et al.* is $\mathbf{z}\|[001]$. In the complete 5L $\mathbf{k}\cdot\mathbf{p}$ model the bands (and consequently the electron spin g^*-factor) are anisotropic. The spherical approximation, which we used above, is obtained by putting the matrix element $Q=0$, see Fig. 1. We also calculated the anisotropic conduction electron g^*-value allowing for $Q\neq 0$ (cf. Ref. 5). After some manipulations the anisotropic correction to g^* for $\mathbf{B}\|[001]$ is obtained in the form

$$\Delta g^*_{001} = \frac{2(2n+1)E_Q\mu_B B}{9}\left[\frac{E_{P_0}}{\tilde{G}_1}\left(\frac{1}{\tilde{E}_0}-\frac{1}{\tilde{G}_0}\right)\left(\frac{7}{\tilde{G}_0}+\frac{5}{\tilde{E}_0}\right) + \frac{E_{P_1}}{\tilde{E}_0}\left(\frac{1}{\tilde{G}_1}-\frac{1}{\tilde{E}_1}\right)\left(\frac{7}{\tilde{E}_1}+\frac{5}{\tilde{G}_1}\right)\right], \tag{A1}$$

where $E_Q=2m_0Q^2/\hbar^2$ and

$$Q=\frac{-i\hbar}{m_0\Omega}\langle X|p_y|Z'\rangle. \tag{A2}$$

The correction to g^*_{001} is manifestly of the nonparabolic character, as it leads to the energy correction $\Delta\mathcal{E}\sim B^2$.

We tried to include the above correction to the description of g^*-factors presented in Fig. 5, taking the value of $E_Q=15.56$ eV (see Ref. 5). However, using our procedure of finding the far-band contribution C' to the g^*- value from other experiments, as described in Sec. II, we found that the modified formula (A1) leads to corrections of C' in such a way that it compensates the above modifications of $g^*(z)$, so that the resulting g^*-values remain virtually unchanged.

Still, we quote the result (A1) as it gives corrections to g^* for $\mathbf{B}\|[001]$ in GaAs-type materials. For the interesting range of $g^*\approx 0$ these corrections are not negligible.

[1] B. E. Kane, Nature (London) **393**, 133 (1998).
[2] D. P. DiVincenzo, J. Appl. Phys. **85**, 4785 (1999).
[3] *Semiconductor Spintronics and Quantum Computation*, edited by D. D. Awschalom, D. Loss, and N. Samarth (Springer-Verlag, Berlin, 2002).
[4] G. Salis, Y. Kato, K. Ensslin, D. C. Driscoll, A. C. Gossard and D. D. Awschalom, Nature (London) **414**, 619 (2001).
[5] P. Pfeffer and W. Zawadzki, Phys. Rev. B **41**, 1561 (1990).
[6] P. Pfeffer and W. Zawadzki, Phys. Rev. B **53**, 12813 (1996).
[7] P. Pfeffer, Phys. Rev. B **59**, 15902 (1999).
[8] P. Pfeffer and W. Zawadzki, Phys. Rev. B **59**, R5312 (1999).
[9] E. L. Ivchenko and A. A. Kiselev, Fiz. Tekh. Poluprovodn. (S.-Peterburg) **26** 1471 (1992) [Sov. Phys. Semicond. **26**, 827 (1992)].
[10] E. L. Ivchenko, A. A. Kiselev and M. Willander, Solid State Commun. **102**, 375 (1997).
[11] A. A. Kiselev, E. I. Ivchenko and U. Roessler, Phys. Rev. B **58**, 16353 (1998).
[12] P. Le Jeune, D. Robart, X. Marie, T. Amand, M. Brousseau, J. Barrau, V. Kalevich and D. Rodichev, Semicond. Sci. Technol. **12**, 380 (1997).
[13] C. Bosio, J. L. Staehli, M. Guzzi, G. Burri and R. A. Logan, Phys. Rev. B **38**, 3263 (1988).
[14] O. Berolo and J. C. Woolley, in *Proceedings of the 11th International Conerence on Physics and Semiconductors* (Polish Scientific Publishers, Warsaw, 1972), p.1420.
[15] B. El Jani, P. Gibart, J. C. Portal, and R. L. Aulombard, J. Appl. Phys. **58**, 3481 (1985).
[16] D. J. Chadi, A. H. Clark, and R. D. Burnham, Phys. Rev. B **13**, 4466 (1976).
[17] C. Weisbuch and C. Hermann, Phys. Rev. B **15**, 816 (1977).
[18] M. Missous, in *Properties of Aluminium Gallium Arsenide*, edited by S. Adachi, Datareviews Series No. 7 (Inspec, 1993), p. 75.
[19] M. Oestreich and W. W. Ruehle, Phys. Rev. Lett. **74**, 2315 (1995).
[20] Y. A. Bychkov and E. I. Rashba, J. Phys. C **17**, 6039 (1984).
[21] G. Dresselhaus, Phys. Rev. **100**, 580 (1955).
[22] W. Zawadzki and P. Pfeffer, Semicond. Sci. Technol. **19**, R1 (2004).
[23] P. Pfeffer and W. Zawadzki, Phys. Rev. B **68**, 035315 (2003).
[24] P. Pfeffer and W. Zawadzki, in *Proceedings of the 23rd International Conference on the Physics of Semiconductors*, edited by M. Scheffer and R. Zimmermann (Springer-Verlag, Berlin, 1996), p. 1815.